Journal of Engineering, Project, and Production Management
2026, 16(7), 2026-0025

Integration of CNN and Attention Mechanism in Fault Identification of Substation Centralized Control Systems

Yi Xia[1], Daojie Pu[2], Cheng Xie[3], Haisheng Jiang[4], Bin Zhang[5], and Yuanyuan Su[6]
[1] Senior Engineer, State Grid Anhui Ultra High Voltage Company, State Grid Anhui Ultra High Voltage Company, Hefei 231131, China, E-mail: xiayilol@163.com (corresponding author).
[2] Senior Engineer, State Grid Anhui Ultra High Voltage Company, China, E-mail: pudj2137@ah.sgcc.com.cn
[3] Senior Engineer, ,State Grid Anhui Electric Power Co., Ltd., China, E-mail: xiec0222@ah.sgcc.com.cn
[4] Senior Engineer, State Grid Anhui Ultra High Voltage Company, China, E-mail: jianghs0551@ah.sgcc.com.cn
[5] Senior Engineer, State Grid Anhui Ultra High Voltage Company, China, E-mail: zhangb647x@ah.sgcc.com.cn
[6] Engineer, State Grid Anhui Ultra High Voltage Company, China

Project Management
Received May 24, 2026; revised June 11, 2026; August 7, 2026; accepted August 11, 2026
Available online August 15, 2026

Abstract: Traditional methods of fault detection do not offer sufficient sensitivity toward significant local characteristics, leaving unsatisfactory results in both detection accuracy and response time. Thus, this article proposes a Convolution Neural Network model with an implementation of a Squeeze-and-Excitation layer, where multi-source time-series sensor data passes through one-dimensional convolutional layer for extracting local features, followed by the global average and pooling of the feature map to get channel statistics, followed by the processing of the information in a dimensionality-reducing fully connected layer with activation through the ReLU function. The dimensionality-increase fully connected layer outputs sigmoid-normalized channel weights. These weights are then multiplied by the original feature map on a channel-by-channel basis; the calibrated features are then fed into a fully connected classification layer to complete fault identification. Results demonstrate a 99.4% recognition accuracy for voltage mutation faults, with an average response time of 47.26ms, validating the key role of this approach in improving the real-time and robustness of power grid fault diagnosis.

Keywords: Substation control system; fault identification; SE module; CNN model; attention mechanism.

DOI 10.32738/JEPPM-2026-0025

---

1. Introduction

As the central hub for power network operations, substation centralized control systems monitor and manage equipment across several stations. Regional power grid stability is directly impacted by its operational status. Traditional monitoring techniques cannot meet the strict safety requirements of contemporary power systems due to the rising number of devices in large-scale power grids and the resulting increased likelihood of failures(Mazhar et al., 2023; Dewangan et al., 2023). Enhancing fault identification capabilities can reduce financial losses and social impacts of widespread power outages and help prevent cascading incidents (Li et al., 2023; Li and Chi, 2024). To ensure grid resilience and continuity of power supply, effective and precise diagnostic mechanisms are of indispensable engineering value (Liao et al., 2023; Mashal, 2023).

Electromagnetic interference reduces the sensor signal-to-noise ratio to below 5 decibels, and conventional methods incur a 3-decibel loss in the feature-extraction signal-to-noise ratio. Because of environmental fluctuations and equipment aging, fault patterns exhibit highly nonlinear characteristics, making it challenging for traditional static models to capture dynamic variations (Ma et al., 2023; Gabriel and Huitink, 2023). Key fault features are easily masked by redundant information, and standard CNNs are unable to dynamically focus on localized abnormal regions during feature extraction (Feng et al., 2023; Zhao et al., 2025). It is challenging to meet system operating standards for fault-identification accuracy and real-time performance due to the combined effects of noise and pattern complexity (Aghazadeh Ardebili et al., 2024; Moysidis et al., 2023).

Threshold discrimination techniques cannot adapt to the changing needs of varying fault scenarios because they rely on empirically determined, fixed thresholds. Although recurrent neural networks, or RNNs, are capable of temporal modeling, their high computational complexity can cause response times to exceed the real-time limitations of centralized control systems (Cao et al., 2024; Pacella et al., 2024). Static bias affects channel weight allocation, and existing attention-mechanism embedding models do not optimize parameters to account for the noisy nature of power data (Liu et al., 2025; Deng et al., 2024). The practical operational requirements of centralized substation control systems cannot be met by fault-identification performance alone, given the limitations of these methods in noisy environments.

The advancements made in deep learning are greatly beneficial in the diagnosis of faults in various industrial applications. Surendran et al. (2022) introduced an innovative industrial fault diagnosis framework involving sailfish-enhanced Inception and residual networks, resulting in impressive results in different datasets relating to bearing and gearbox devices. Tamilvizhi and Surendran (2020) came up with an ewfficient method of dealing with unhealthy resources with regard to proactive fault tolerance in cloud computing applications. Tamilvizhi et al. (2025) used machine learning models to assess the lifespan of power transformers by taking into account working conditions and other factors, thus involving the possibility of preventive maintenance. Ramya et al. (2025) suggested a more secure version of a cloud security framework, which draws on multi-factor authentication and the three-level access control approach, thus applying an improved double-layer encryption framework. These recent studies address fault identification, resource recovery, lifetime estimation, and secure access in related technical domains, providing methodological references for the design of the proposed SE-CNN model for centralized control systems in substations.

To create a feature-processing framework with channel-wise adaptive capabilities, this paper closely couples the SE module with a one-dimensional convolutional neural network, thereby addressing inaccurate feature extraction in fault identification for centralized control systems in substations. By statistically evaluating global features and modeling channel relationships to dynamically adjust each channel's response strength, this architecture overcomes the shortcomings of traditional CNNs in detecting local anomalies. In contrast to the current attention mechanisms, the method proposed here employs a dynamic allocation of weights, allowing the odality of the features to be changed. As a result, it contributes to a higher level of accuracy in the identification of severe malfunction in complex electromagnetic environment. The research is aimed at three inquiries. The first one concerns the creation of a method for the calibration of the channels for extracting malfunction characteristics under electromagnetic noise. The second question is about the verification of the robustness of the SE-CNN. The last query is whether the time of inference is suitable for the needs of the centralized substations' control system.

In comparison to fixed-threshold approaches such as recurrent neural networks and conventional convolutional networks, the proposed model offers a new mechanism for channel-wise adaptive weight assignment to cope with the issues of static bias and noise interference as well as a parameter optimization for noise-affected power data.

2. Design of CNN Fault Recognition Model Integrating Attention Mechanism

A theoretical framework grounded in channel attention mechanisms and feature recalibration guides the model's design. The framework formulates fault identification as a sequential process: noise-robust feature derivation from multi-source temporal data, adaptive weighting of channel-wise feature responses, and classification using recalibrated feature representations. This framework transforms raw sensor signals into discriminative fault patterns through a four-stage pipeline comprising wavelet-based preprocessing, one-dimensional convolutional feature extraction, squeeze-and-excitation-based channel calibration, and fully connected classification.

2.1. Data Preprocessing for Time Series Fault Data

In environments with high electromagnetic interference, multi-source time-series sensor data from centralized substation control systems exhibit notable data drift. The feature extraction process is severely hampered by contamination of the original signal with high-frequency random noise and low-frequency baseline drift. The original time-series signal is decomposed into frequency subbands using a discrete wavelet transform to handle the distinct noise-distribution properties of power systems (Sinha et al., 2025; Priyadarshini et al., 2025; Latif et al., 2024). The threshold parameter is adaptively determined by the wavelet threshold denoising process according to the noise level and signal length (Halidou et al., 2023; Yang et al., 2023; Zhu et al., 2024).

$$\lambda = \sigma\sqrt{2\log N} \tag{1}$$

In Eq. (1), λ represents the wavelet threshold, σ is the noise standard deviation, and N is the time series signal length. This threshold is applied to hard thresholding of the wavelet coefficients, retaining coefficients with absolute values greater than the threshold and setting the remaining coefficients to zero. A five-layer wavelet decomposition structure is used, with Daubechies 4 (db4) as the mother wavelet function, to ensure that the fault signature information is retained while effectively suppressing noise interference.

Table 1. Key parameter settings for data preprocessing

Parameter items	Numerical	Unit
Sampling frequency	10	kHz
Sliding window length	256	Sampling point
Sliding step length	64	Sampling point
Wavelet decomposition level	5	Layer
Mother wavelet function	db4	-
Noise reduction threshold coefficient	0.6745	-

In Table 1, a 10kHz sampling frequency meets the requirements for power signal feature extraction. A sliding window length of 256 sampling points and a sliding step size of 64 sampling points ensure continuity of time series features. A five-layer wavelet decomposition structure balances feature preservation and computational efficiency. The db4 mother wavelet function adapts to the characteristics of power transient signals, and a threshold coefficient of 0.6745 is calculated based on the noise statistics of the detail coefficients in the first layer of the wavelet decomposition. All parameter values meet the engineering constraints for real-time substation fault diagnosis.

The dataset comprises 100,000 time-series samples at a 10 kHz sampling rate, covering five fault categories with 20,000 samples each, sourced from measured and simulated data of a substation centralized control system.

The preprocessed time series data is segmented using a sliding window mechanism, with each window containing time series data collected synchronously from multiple sensors, such as voltage and current. Z-score normalization is performed independently within each sliding window to eliminate the impact of differences in sensor data magnitude on subsequent feature extraction (Chen et al., 2024; Guo et al., 2024).

$$Z = \frac{x_1 - \mu}{\sigma_1} \tag{2}$$

In Eq. (2), Z represents the standardized data, x_1 is the original data value, μ is the mean of the feature dimension, and σ_1 is the standard deviation of the feature dimension.

2.2. CNN Fusion Architecture Based on SE Attention Mechanism

The CNN model described in this section takes the input of processed multi-source time-series sensor data and produces a probability distribution covering five fault categories. The architecture consists of three convolutional layers to extract local features. The input of the first convolutional layer has a kernel size of 15 while the kernel size of the second and third layers decreases to 9 and 5 respectively. The stride value for all the convolutional layers is set into 2, with the number of convolutional kernels identified as 64, 128, and 256 for the first, second, and third layer respectively. After applying convolution on the input data, the Batch Normalization layer and Rectified Linear Unit (ReLU) activation function are used to extract the features (Taye, 2023; Usman et al., 2025). In addition, the output from the third convolutional layer is processed via a channel attention mechanism utilizing the Squeeze-and-Excitation (SE) module, which consists of three components of processing called squeeze and excitation along with feature calibration (Ruifeng et al., 2024; Nisar et al., 2023).

The squeeze operation compresses each channel's feature map into a single scalar value via global average pooling. For the input feature map $F \in \mathbb{R}^{C\times T}$, where C represents the number of channels and T represents the length of the time series, the global average pooling operation is expressed as (Xu et al., 2023; Kim et al., 2023).

$$z_c = \frac{1}{T}\sum_{t=1}^{T} F_c(t) \tag{3}$$

In Eq. (3), z_c represents the global statistics of the c-th channel and $F_c(t)$ represents the eigenvalue of the c-th channel at the time point t. This operation converts the two-dimensional feature map into a one-dimensional channel description vector $z \in \mathbb{R}^{C}$.

The excitation operation builds channel dependencies through two fully connected layers. The first fully connected layer compresses the channel dimension to 1/16 of the original size, with a compression ratio of $r = 16$, and the second layer restores it to the original number of channels. Assuming the weight matrix of the first fully connected layer is $W_1 \in \mathbb{R}^{(C/r)\times C}$, and the weight matrix of the second fully connected layer is $W_2 \in \mathbb{R}^{C\times(C/r)}$, then the channel weight vector $s \in \mathbb{R}^{C}$ The calculation formula for the output of the excitation operation is shown in Eq. (4).

$$s = \sigma_2\big(W_2 \cdot \delta(W_1 \cdot z)\big) \tag{4}$$

In Eq. (4), the term σ_2 symbolizes the Sigmoid activation function, whereas the term delta represents the ReLU activation function. In this context, W_1 and W_2 refer to the weight matrices of the dimensionality reduction and dimensionality expansion layers, respectively. The s produced in this process represents the significance distribution for each channel. The calibrated feature map is obtained by multiplying s with the original feature map F, leading to the generation of the output feature map F' . The final result, which is the fault classification, is achieved by passing the calibrated feature map through two fully connected layers and the Softmax classifier.

Fig. 1 shows the complete process of the SE-CNN fusion architecture, highlighting the branching structure of the SE module and its integration with the CNN backbone network.

As shown in Fig. 1, this design demonstrates the major operation of SE-CNN: there are 3 layers of convolution followed by batch normalization and ReLU activation function. The output of the third layer enters the SE block and the feature recalibration process simultaneously. In the SE block, global average pools are performed and the channels are compressed and restored before utilizing Sigmoid function. Channel importance weights are applied to the input feature map at the channel level, completing the recalibration process before classifying the features.

The distinction of the SE module from the general one-dimensional CNN is attributed to its utilization of an adaptive weight distribution system along the channel dimension that allows the network the flexibility to modulate the strength of the response of each channel features. The workflow of the SE-CNN algorithm is illustrated in the following order. Initially, multi-source time-series data that has undergone preprocessing is sent to the three-layer one-dimensional convolutional system for local feature extraction. Then, the generated feature map undergoes global average pooling to create a channel descriptor vector. Afterwards, a fully connected layer that has dimensionality compression with ReLU activation follows this by a dimensionality-increasing fully connected layer with sigmoid activation to produce the normalized channel weights. These weights multiplied with the original feature map yield calibrated features that finally pass through two fully connected layers to be classified by Softmax.

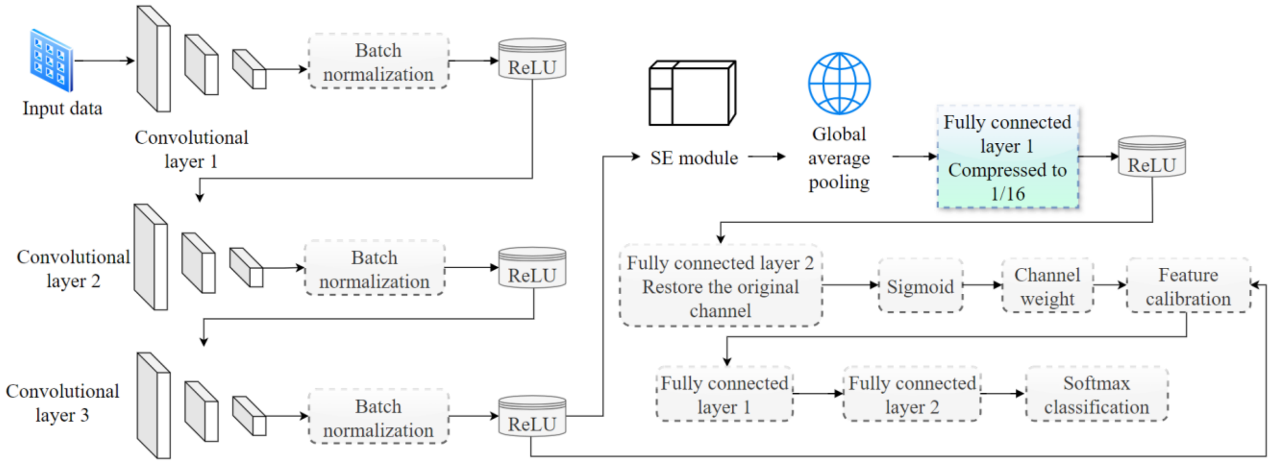

Fig. 1. Schematic diagram of SE-CNN fusion architecture

2.3. Characteristic Calibration Mechanism for Power Noise

The feature calibration mechanism receives as input the channel weight vector generated by the excitation operation, which is processed byσ_2 to obtain the normalized weight distribution. σ_2 maps any real number to the interval (0,1), which is mathematically expressed as shown in Eq. (5).

$$\sigma_2(x) = \frac{1}{1+e^{-x}} \tag{5}$$

In Eq. (5), x represents the real value of the input, e is the base of the natural logarithm. The output of this function is strictly constrained to the open interval (0, 1), ensuring that each channel's weight has clear upper and lower bounds. Each element s_c of the weight vector s corresponds to the c-th channel of the original feature map F, indicating the channel's relative importance.

The calibration operation is performed by element-wise multiplication of the channel weight vector by the original feature map. The calculation formula of the calibrated feature map is:

$$F_{c,t}^{'} = s_c \cdot F_{c,t} \tag{6}$$

In Eq. (6), c represents the channel index, t represents the time series position, s_c represents the weight value of the c-th channel, and $F_{c,t}$ represents the feature value of the original feature map at the channel c and time point t.

The weight vector establishes dependencies between channels through learning, assigning lower weights to channels with noise information and higher weights to channels with significant fault signatures. In electromagnetic interference environments, the weight vector dynamically adjusts the contribution ratio of each channel, allowing the feature representation to focus more on the discriminative elements of the signal (Rong et al., 2025; Song et al., 2025).

3. Experiment and Results Analysis

3.1. Experiment

In this research, five different faults are featured, and their identification performance is assessed using a confusion matrix, the duration of response is obtained to ensure that system works under real-time conditions, and finally, the electromagnetic interference gradient test is performed to assess the reliability of the process.

Experimental research has been implemented in a high-performance computing facility where NVIDIA Tesla V100 GPU served as computing hardware used for model training and experimental validation in TensorFlow 2.6.0 environment. Moreover, the whole experimentation was performed in the operating system Ubuntu 18.04 to enable multithreaded data processing. All experiments were conducted on a Linux system that allowed for development of the optimal preprocessing and training technique. All data were captured simultaneously from multiple sources at the speed of 10 kHz and converted into segments for usage in the model.

Table 2 includes five fault categories, with 20,000 samples for each category to ensure data balance. The sampling frequency is 10 kHz, meeting the requirements for power system fault pattern recognition. Each fault category accounts for 20% of the total, ensuring that all fault types are fully represented during training. Table 3 lists five example samples with the first five sampling points of each 256-point time-series segment.

Table 2. Basic statistical information

Parameter items	Numerical	Unit
Sample size	100,000	-
Sampling frequency	10	kHz
Fault Category	5	-
The proportion of each type of failure	20%	-
The amount of data per category	20,000	-

Table 3. Example samples from the dataset

Sample Index	Time-Series Segment Values (first 5 of 256 points)	Fault Category
1	[1.24, -0.58, 2.31, -1.02, 0.87]	Short-circuit fault
2	[0.32, -0.15, -2.18, 0.76, -0.44]	Grounding fault
3	[-0.87, 1.56, -3.42, 2.89, -1.23]	Voltage mutation fault
4	[0.56, 0.61, 0.59, 0.63, 0.55]	Overload fault
5	[-0.12, -0.08, -0.15, 0.09, 0.11]	Equipment abnormality fault

3.2. Multi-dimensional Performance Evaluation on Five Fault Categories

In order to solve the problem that the characteristics of multiple types of faults in the fault identification of substation centralized control system are significantly different, and the noise interference is complex, the study adopts the confusion matrix method to systematically analyze the SE-CNN discrimination characteristics of five typical faults (Najafzadeh et al., 2024; Yaacoub et al., 2025). Of all faults mentioned, short-circuit ones are identified by instant increments of current, ground faults by abnormal fluctuations of phase, voltage mutations by evident mutations at local level, overload faults by continuous amplitude deviations, and abnormal faults by abnormal but clinically useful trends of faults; recognition accuracy shows the performance level of the model as suggested by its discriminating power, precision shows the reliability of fault group assessment, and recall assesses the model's performance with respect to real faults. F1-score is computed as the product of precision and recall multiplied by 2 and divided by the result by their sum. The model's discrimination across fault categories is cross-validated using multi-dimensional indicators (Chen et al., 2024), as shown in Fig. 2.

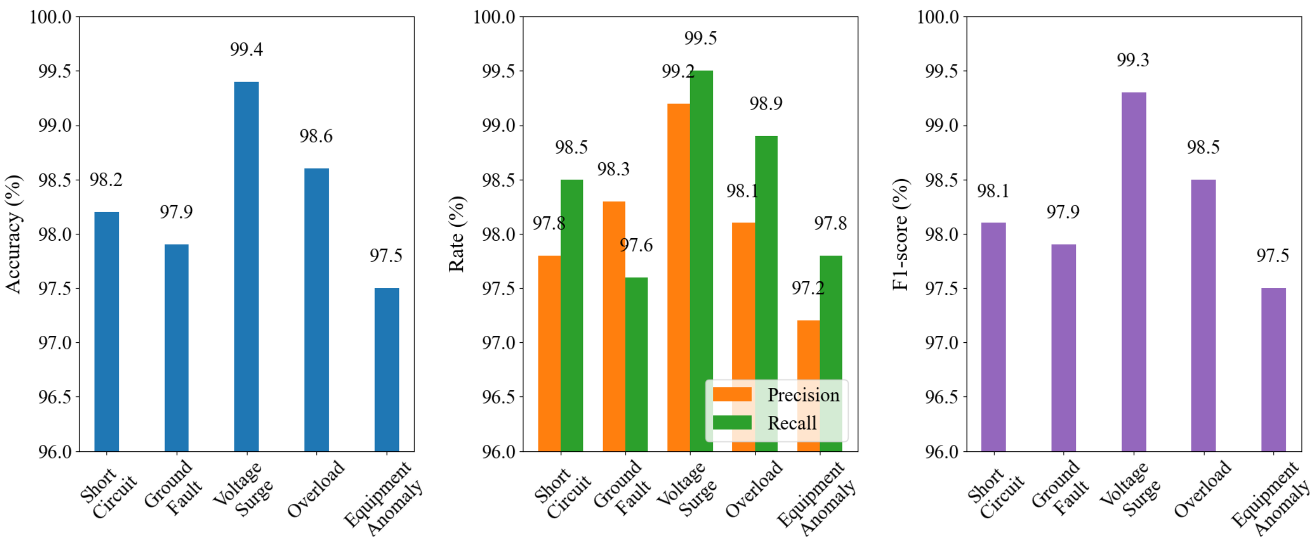

(a) Recognition accuracy (b) Precision vs. recall (c) F1-score distribution

Fig. 2. Multi-dimensional performance evaluation of CNN model integrated with SE module on five types of faults

As shown in Fig. 2, the recognition accuracy for voltage mutation faults reaches 99.4%, with a precision 99.2% and a recall 99.5%, maintaining a high balance. The accuracy rates for short-circuit and overload faults are 98.2% and 98.6%, respectively, with F1 scores of 98.1% and 98.5%. Ground faults have an accuracy of 98.3%, which is somewhat greater than the recall rate of 97.6%. The accuracy and the F1 score of abnormal equipment faults is 97.5%, the smallest among the five fault types. The varying values of precision and recall scores for each fault type show the objective differences in the model's discrimination ability about the fault characteristics.

3.3. Response Time and Overhead Evaluation

The requirement of having a high level of certainty in dealing with faults in centralized control systems is vital. The purpose of this paper is to evaluate the timing of the identification process of five common faults. The identification monitoring of failures is called the response time and is vital for analyzing the performance of any system. Furthermore, when it comes to the evaluation of the channel attention technology's efficiency, the additional load that the SE module brings into account plays an essential role. Meanwhile, even if the nature of some faults such as voltage mutation ones makes it easier to identify them quickly, there could be delays in the operation in the case of equipment fault. Fig. 3 compares the response time of a standard CNN and a fused SE-CNN for five fault types, as well as the distribution of the additional time applied by the SE module.

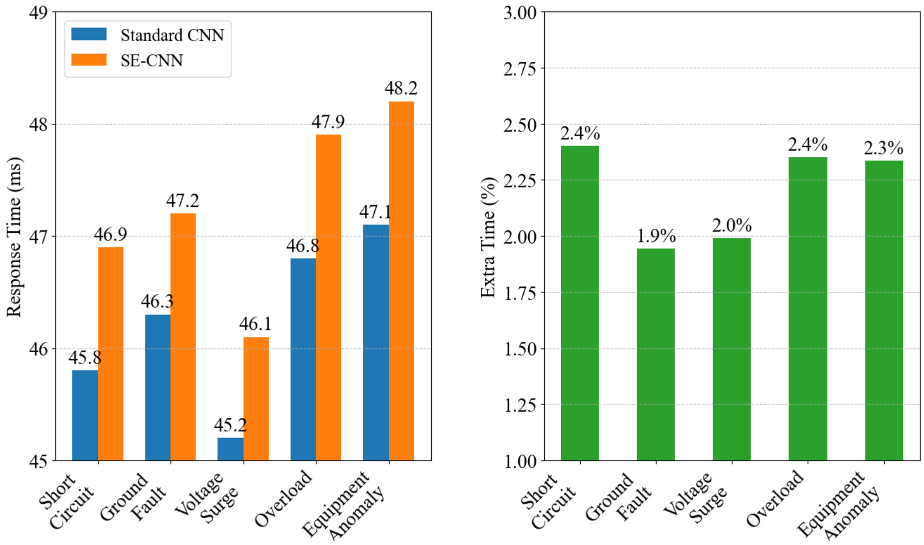

(a) Response time comparison (b) SE module overhead

Fig. 3. Comparison of response time and overhead of CNN integrated with SE module for five types of faults

In Fig. 3, the average response times for the standard CNN and SE-CNN are 46.24ms and 47.26ms, respectively, with an average latency increase of 1.02ms. Voltage mutation faults have the shortest response time, at 45.2ms for the standard CNN and 46.1ms for the SE-CNN. These faults have distinct characteristics and are easy to identify. Equipment abnormality faults have the longest processing time, at 47.1ms for the standard CNN and 48.2ms for the SE-CNN. These faults have high feature complexity and relatively low recognition accuracy. The SE module adds 1.9% to 2.4% processing time. Ground faults add 1.9% to processing time, while short-circuit and overload faults add 2.4%. These differences arise from the SE module's adaptive weight allocation mechanism across fault-feature channels.

3.4. Verification of Robustness in Noisy Environments

To conduct the experiment, a testing environment with electromagnetic interference sensitivity that varies from 0% to 100% is created in order to test if the SE module is able to perform feature correction using the CNN model in the substation ECS. A reliable feature extraction system is necessary because different fault effects produce different sensitivity to noise level. It is by considering the standard deviation of the calibrated feature vector that the stability of the characteristics is evaluated in the noise environment and the power of the model against noise is determined. The ability of the SE module to adapt dynamically to the noise levels is characterized by the cosine criterion between channel weight vector and the noise-free vector. Fig. 4 illustrates the trend in the performance of the feature correction from the SE-CNN model in relation to electromagnetic interference level.

As depicted in Fig. 4, the standard deviation of the calibrated feature vectors continues to rise from 1.23×10^{-3} to 5.82×10^{-3} as the intensity of electromagnetic interference gradually increases, moving from zero to full load. The standard deviation increases by 1.57×10^{-3} in the range of electromagnetic interference intensity from 75% to 100%, which is more than in the previous stages. These results indicate that the stability of the features starts to fall very quickly once the intensity of noise interference reaches some level. Given that the cosine similarity of the channel weight vector with initial value of 1.00 becomes 0.65 at the interference-free baseline and then returns to 0.88 at interference intensity of 50%, it can be concluded that the SE module selects important feature channels in moderate interference conditions. The combined impact of stability of the feature vector and ability of the CNN equipped with the SE module to adjust weights dynamically makes it possible to represent fault features properly under very strong electromagnetic interference conditions.

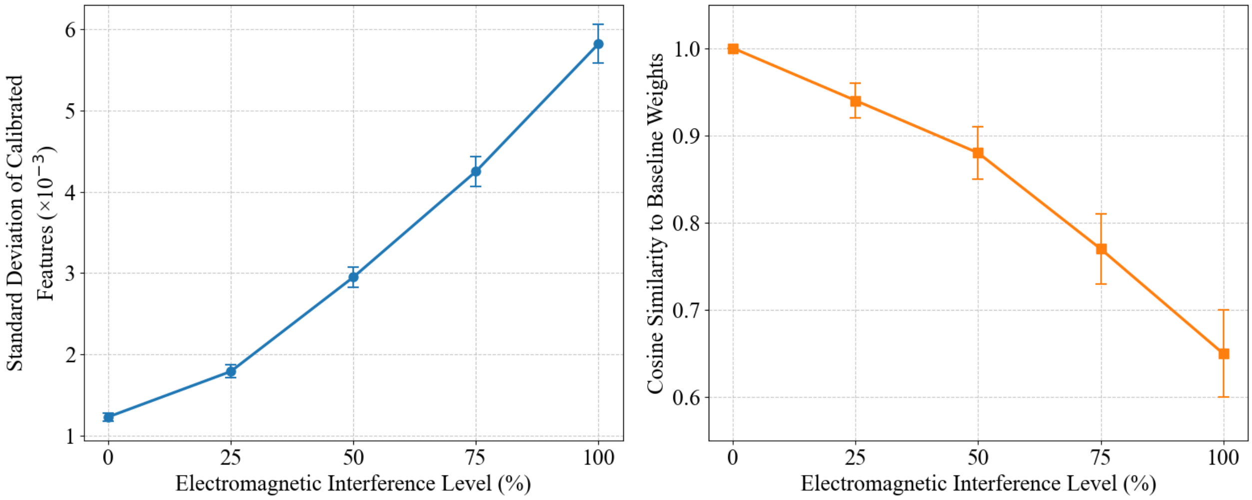

(a) Feature Vector Stability (b) Weight Vector Adaptation

Fig. 4. Stability analysis of feature calibration mechanism under electromagnetic interference

4. Conclusion

This paper proposes a CNN integrated with a squeeze-and-excitation module for fault identification in centralized control systems for substations. The model extracts local features from multi-source time-series sensor data using one-dimensional convolutional layers, computes channel statistics via global average pooling, and outputs sigmoid-normalized channel weights via dimensionality-reduced and restored fully connected layers. A dynamic calibration mechanism performs weighted fusion of feature maps on a per-channel basis. Experimental results demonstrate 99.4% recognition accuracy for voltage-mutation faults, up from 96.8% for a standard convolutional network. The average response times of the standard CNN and the proposed SE-CNN are 46.24 milliseconds and 47.26 milliseconds, respectively, with the additional time from the SE module kept within 2.4 percent. The proposed model reduces the growth rate of the standard deviation of the feature vector under electromagnetic interference by approximately 30 percent.

The theoretical implication is the validation of channel-wise attention mechanisms for noise-robust feature calibration in power system fault diagnosis. The practical implication for engineers is a fault-identification model that can be applied to meet the latency requirements of substation automation systems. The model is utilized by system operators to prioritize the real-time notifications of voltage fluctuations and short-circuit faults, redirecting the diagnostic efforts from threshold-based techniques to attention-based classification. The performance of the model reaches an accuracy of 97.5% in achieving faults related to abnormal operation of the equipment, which indicates the low discrimination power of the model concerning gradual or unexpected faults. The model relies heavily on high-quality labeled data. The future research will be focused on developing a lighter architecture for a reduced channel-attention overhead as well as employing semi-supervised learning methods for better utilization of the limited volume of labeled data.

Author Contributions

Yi Xia contributed to conceptualization, project administration, supervision, funding acquisition, and manuscript review and editing. Daojie Pu contributed to conceptualization, methodology design, supervision, validation, and funding acquisition. Cheng Xie contributed to formal analysis, investigation, data curation, draft preparation, and data analysis. Haisheng Jiang contributed to resource provision, data collection, validation, and technical support. Bin Zhang contributed to manuscript review and editing, visualization, validation, and technical guidance. Yuanyuan Su contributed to software implementation, investigation, draft preparation, visualization, and data preprocessing. All authors have read and agreed with the manuscript before its submission and publication.

Funding

This research received no specific financial support from any funding agency.

Institutional Review Board Statement

Not applicable.

Declaration of Artificial Intelligence (AI) Tools

The authors used Deepseek solely for language editing and readability improvement. The authors reviewed and verified all content and take full responsibility for the accuracy and integrity of the manuscript.

References

Aghazadeh Ardebili, A., Hasidi, O., Bendaouia, A., Khalil, A., Khalil, S., Luceri, D., Longo, A., Abdelwahed, E. H., Qassimi, S., and Ficarella, A. (2024). Enhancing resilience in complex energy systems through real-time anomaly detection: a systematic literature review. *Energy Informatics,* 7(1), 96-135. doi: 10.1186/s42162-024-00401-8

Cao, K., Zhang, T., and Huang, J. (2024). Advanced hybrid LSTM-transformer architecture for real-time multi-task prediction in engineering systems. *Scientific Reports,* 14(1), 4890-4913. doi: 10.1038/s41598-024-55483-x

Chen, X., Godin, N., Doitrand, A., and Fusco, C. (2024). Reduction in the sensor effect on acoustic emission data to create a generalizable library by data merging. *Sensors,* 24(8), 2421-2442. doi: 10.3390/s24082421

Chen, X., Wang, M., and Zhang, H. (2024). Machine learning-based fault prediction and diagnosis of brushless motors. *Engineering Advances,* 4(3), 130-142. DOI: 10.26855/ea.2024.07.004.

Deng, Y., Liu, J., Zhu, K., Xie, Q., and Liu, H. (2024). PMSNet: Multiscale partial-discharge signal feature recognition model via a spatial interaction attention mechanism. *Sensors,* 24(11), 3342-3361. doi: 10.3390/s24113342

Dewangan, F., Abdelaziz, A. Y., and Biswal, M. (2023). Load forecasting models in smart grid using smart meter information: A review. *Energies,* 16(3), 1404-1458.doi: 10.3390/en16031404

Feng, Z., Li, Y., Sun, B., and Yang, C. (2023). Abnormal operating condition identification of industrial processes based on deep learning with global-local slow feature analysis. *IEEE Transactions on Instrumentation and Measurement*, 72, 1-11.doi: 10.1109/TIM.2023.3267347

Gabriel, O. E., and Huitink, D. R. (2023). Failure mechanisms driven reliability models for power electronics: A review. *Journal of Electronic Packaging,* 145(2), 020801-020825. doi: 10.1115/1.4055774

Guo, J., Wei, J., Xiang, Y., and Han, C. (2024). Millimeter-wave radar-based identity recognition algorithm built on multimodal fusion. *Sensors,* 24(13), 4051-4074. doi: 10.3390/s24134051

Halidou, A., Mohamadou, Y., Ari, A. A. A., and Zacko, E. J. G. (2023). Review of wavelet denoising algorithms. *Multimedia Tools and Applications,* 82(27), 41539-41569.doi: 10.1007/s11042-023-15127-0

Kim, J. S., Park, S. W., Kim, J. Y., Park, J., Huh, J. H., Jung, S. H., and Sim, C. B. (2023). E-hrnet: Enhanced semantic segmentation using squeeze and excitation. *Electronics,* 12(17), 3619-3634. doi: 10.3390/electronics12173619

Latif, I. H., Abdulredha, S. H., and Hassan, S. K. A. (2024). Discrete wavelet transform-based image processing: A review. *Al-Nahrain Journal of Science,* 27(3), 109-125.doi: 10.22401/ANJS.27.3.13

Li, M. J., and Chi, K. T. (2024). Quantification of cascading failure propagation in power systems. *IEEE Transactions on Circuits and Systems I: Regular Papers,* 71(8), 3717-3725.doi: 10.1109/TCSI.2024.3383450

Li, M. J., Tse, C. K., Liu, D., and Zhang, X. (2023). Cascading failure propagation and mitigation strategies in power systems. *IEEE Systems Journal,* 17(2), 3282-3293.doi: 10.1109/JSYST.2023.3248044

Liao, C., Li, Y., Ma, J., Zhou, N., Yu, H., Cao, Y., and Rehtanz, C. (2023). A resilience evaluation method considering power source ability and network topology of power systems. *IEEE Systems Journal,* 17(3), 3527-3538.doi: 10.1109/JSYST.2023.3273922

Liu, B., Wang, X., Zhang, Z., Zhao, Z., Wang, X., and Liu, T. (2025). Fault Prediction of Hydropower Station Based on CNN-LSTM-GAN with Biased Data. *Energies,* 18(14), 3772-3792. doi: 10.3390/en18143772

Ma, N., Yang, D., Riaz, S., Wang, L., and Wang, K. (2023). Aging mechanism and models of supercapacitors: A review. *Technologies,* 11(2), 38-52. doi: 10.3390/technologies11020038

Mashal, I. (2023). Smart grid reliability evaluation and assessment. Kybernetes, 52(9), 3261-3291.doi: 10.1108/K-12-2020-0910

Mazhar, T., Irfan, H. M., Khan, S., Haq, I., Ullah, I., Iqbal, M., and Hamam, H. (2023). Analysis of cyber security attacks and its solutions for the smart grid using machine learning and blockchain methods. *Future Internet,* 15(2), 83-119.doi: 10.3390/fi15020083

Moysidis, D. A., Karatzinis, G. D., Boutalis, Y. S., and Karnavas, Y. L. (2023). A study of noise effect in electrical machines bearing fault detection and diagnosis considering different representative feature models. *Machines*, 11(11), 1029-1057. doi: 10.3390/machines11111029

Najafzadeh, M., Pouladi, J., Daghigh, A., Beiza, J., and Abedinzade, T. (2024). Fault detection, classification and localization along the power grid line using optimized machine learning algorithms. *International Journal of Computational Intelligence Systems,* 17(1), 49-66. doi: 10.1007/s44196-024-00434-7

Nisar, M. Z., Ibrahim, M. S., Usman, M., and Lee, J. A. (2023). A lightweight deep learning model for automatic modulation classification using residual learning and squeeze – excitation blocks. *Applied Sciences,* 13(8), 5145-5162. doi: 10.3390/app13085145

Pacella, M., Papa, A., and Papadia, G. (2024). On integrating time-series modeling with long short-term memory and Bayesian optimization: a comparative analysis for photovoltaic power forecasting. *Applied Sciences,* 14(8), 3217-3236. doi: 10.3390/app14083217

Priyadarshini, M. S., Bajaj, M., and Zaitsev, I. (2025). Energy feature extraction and visualization of voltage sags using wavelet packet analysis for enhanced power quality monitoring. *Scientific Reports*, 15(1), 2226-2252. doi: 10.1038/s41598-025-86126-4

Ramya, M., Tamilvizhi, T., and Navaneethakrishnan, S. R. (2025, September). Enhancing cloud security with multi-factor authentication and optimized encryption algorithm. *In 2025 6th International Conference on Electronics and Sustainable Communication Systems (ICESC),* 1033-1039). IEEE.DOI: 10.1109/ICESC65114.2025.11212624

Rong, Y., Wang, A., Wang, M., and Zhu, T. (2025). Adaptive signal recognition in mines based on deep learning. *Scientific Reports,* 15(1), 10245-10267. doi: 10.1038/s41598-025-95070-2

Ruifeng, D., Yuanlin, Z., Haiyan, Z., Xinze, L., Peng, C., and Yonghui, L. (2024). A high resolution convolutional neural network with squeeze and excitation module for automatic modulation classification. China Communications, 21(10), 1-16.doi: 10.23919/JCC.ja.2022-0270

Sinha, P., Paul, K., Snehalika, S., Kasireddy, I., Krishna, A. B., Naga Malleswara Rao, D. S., Shuaibu, H. A., and Ustun, T. S. (2025). Multiscale detection of power quality disturbances and cyber intrusions in smart grids using NSCT and frequency band scalograms. *Scientific Reports,* 15(1), 32375-32395. doi: 10.1038/s41598-025-18127-2

Song, Q., Sun, S., Song, Q., Wang, B., Liu, Z., and Jiang, H. (2025). A deep learning method based on multi-scale fusion for noise-resistant coal-gangue recognition. *Scientific Reports,* 15(1), 101-118. doi: 10.1038/s41598-024-83604-z

Surendran, R., Khalaf, O. I., and Tavera Romero, C. A. (2022). Deep learning based intelligent industrial fault diagnosis model. *Computers, Materials and Continua,* 70(3), 6323-6338.DOI:10.32604/cmc.2022.021716

Tamilvizhi, T. and Surendran, R. (2020). Time and cost-effective recovery mechanism for unhealthy resources in proactive fault tolerance framework. *In IET Conference Proceedings CP777,* 6, 444-449. Stevenage, UK: The Institution of Engineering and Technology .https://doi.org/10.1049/icp.2021.075

Tamilvizhi, T., Shivani, S., and Thabiba, B. (2025). Longevity of Power Transformers Developing ML a for Accurate Lifetime Estimation. *In 2025 2nd International Conference on Computing and Data Science (ICCDS),* 1-5. IEEE.DOI: 10.1109/ICCDS64403.2025.11209731

Taye, M. M. (2023). Theoretical understanding of convolutional neural network: Concepts, architectures, applications, future directions. *Computation,* 11(3), 52-74. doi: 10.3390/computation11030052

Usman, O. L., Muniyandi, R. C., Omar, K., Mohamad, M., Owoade, A. A., and Kareem, M. A. (2025). HoRNS-CNN model: an energy-efficient fully homomorphic residue number system convolutional neural network model for privacy-preserving classification of dyslexia neural-biomarkers. *Brain Informatics,* 12(1), 11-38. doi: 10.1186/s40708-025-00256-z

Xu, S., Zhang, L., Tang, Y., Han, C., Wu, H., and Song, A. (2023). Channel attention for sensor-based activity recognition: Embedding features into all frequencies in DCT domain. *IEEE Transactions on Knowledge and Data Engineering,* 35(12), 12497-12512.doi: 10.1109/TKDE.2023.3277839

Yaacoub, J. P. A., Noura, H. N., Salman, O., and Chahine, K. (2025). Toward secure smart grid systems: risks, threats, challenges, and future directions. *Future Internet,* 17(7), 318-404. doi: 10.3390/fi17070318

Yang, W., Chen, B., Shen, Y., and Yu, L. (2023). WaveCNNs-AT: Wavelet-based deep CNNs of adaptive threshold for signal recognition: W. Yang et al. *Applied Intelligence,* 53(23), 28819-28831.doi: 10.1007/s10489-023-05047-9

Zhao, H., Fan, Y., Ma, J., Wu, Y., Qin, N., Wang, H., Zhu, J., and Deng, A. (2025). Fault Diagnosis of Rolling Bearing Based on Spectrum-Adaptive Convolution and Interactive Attention Mechanism. *Machines,* 13(9), 795-817. doi: 10.3390/machines13090795

Zhu, G., Liu, B., Yang, P., and Fan, X. (2024). Image denoising method based on improved wavelet threshold algorithm. *Multimedia Tools and Applications,* 83(26), 67997-68011.doi: 10.1007/s11042-024-18197-w

Yi Xia was born in Chaohu, Anhui. P.R. China, in 1989. He received his master’s degree from Hefei University of Technology, P.R. China. He currently works at State Grid Anhui Ultra High Voltage Company. His research interests include electric power system automation, centralized monitoring and control systems for substations, and cybersecurity of power systems.

Daojie Pu was born in Huoqiu, Anhui. P.R. China, in 1983. He received the master's degree from Hefei University of Technology, P.R. China. Now, he works at State Grid Anhui Ultra High Voltage Company. His research interests include electric power system automation and power substation maintenance.

Xie Cheng was born in Tongcheng, Anhui. P.R. China, in 1993. She earned her master’s degree from the University of Science and Technology of China. She currently works at State Grid Anhui Electric Power Co., Ltd. Her research interests include electric power systems and their automation, as well as automatic control engineering.

Haisheng Jiang was born in Xuancheng, Anhui. P.R. China, in 1973. He received his bachelor's degree from Hefei University of Technology, P.R. China. Now, he works at State Grid Anhui Ultra High Voltage Company. His research interests focus on relay protection in electric power systems, substation operation and maintenance.

Bin Zhang was born in Suzhou, Anhui. P.R. China, in 1987. He received his bachelor's degree from China University of Mining and Technology, P.R. China. Now, he works at State Grid Anhui Ultra High Voltage Company. His research interests focus on substation operations and maintenance, and centralized monitoring and control systems for substations.

Yuanyuan Su was born in Shucheng, Anhui. P.R. China, in 1992. She received the master's degree from Hefei University of Technology, P.R. China. Now, he works at State Grid Anhui Ultra High Voltage Company. Her research interests include electric power system automation and power substation maintenance.